

Original Research Articles

Molecular cloning and expression profiles of MnSOD and CAT genes from the turbot *Scophthalmus maximus*

Hai Ren^{1,2a}, Qinglin Wang^{1,2,3}, Xiaomin Jin^{1,2}, Guisheng Gao^{1,2}, Jing Mei², Guoshan Qi², zenping He², Shaoyu Yang^{4b}¹ Hebei Key Laboratory of Ocean Dynamics, Resources and Environments, Hebei Normal University of Science and Technology, Qinhuangdao, 066004, China, ² College of Marine Resources and Environment, Hebei Normal University of Science and Technology, Qinhuangdao, 066004, China,³ Marine Living Resources and Environment Key Laboratory of Hebei Province, Qinhuangdao, 066004, China, ⁴ Guangxi Key Laboratory of Beibu Gulf

Marine Biodiversity Conservation, College of Marine Sciences, Beibu Gulf University, Qinzhou, 535011, China

Keywords: catalase, manganese superoxide dismutase, *Scophthalmus maximus*, transcriptional analysis, *Vibrio anguillarum*<https://doi.org/10.46989/001c.82198>

Israeli Journal of Aquaculture - Bamidgheh

Vol. 75, Issue 2, 2023

Manganese superoxide dismutase (MnSOD) and catalase (CAT) could eliminate reactive oxygen species (ROS) and maintain the reduction-oxidation balance in cells. This study aimed to investigate their functions in turbot (*Scophthalmus maximus*) response to the *Vibrio anguillarum* challenge. SmMnSOD, the full-length liver cDNA of MnSOD from *S. maximus*, was cloned by fast amplification of cDNA ends (RACE). Sequencing of nucleotides indicated that the SmMnSOD cDNA was 1267 base pairs with a 684-base-pair open reading frame, encoding a 228 amino acid protein with 28 amino acid residues. The SmMnSOD sequence contains MnSOD signatures (DVWEHAYY) and probable N-glycosylation sites (NVT, NHT, and NLS). The deduced sequence of SmMnSOD revealed sequence homology between 85.3% and 92.9% with those of other species. A phylogenetic study found that SmMnSOD clustered with other fish MnSOD, indicating that SmMnSOD was a member of the MnSOD family. The SmMnSOD transcript was discovered by qRT-PCR in the gill, stomach, head-kidney, muscle, liver, intestine, and heart of *S. maximus*, with the highest expression in the liver. Upon intervention by *V. anguillarum*, the liver and head kidney transcript levels of SmMnSOD were up-regulated at 12 and 48 h, whereas the temporal expression profiles of the CAT transcript increased at 6 and 24 h. As the pathogenic bacterial stress processing was prolonged to 72 h, the liver and head kidney transcript levels of SmMnSOD and CAT decreased gradually. Thus, SmMnSOD was triggered and may be related to *S. maximus*' immunological responses against *V. anguillarum*.

INTRODUCTION

Reactive oxygen species (ROS, such as O²⁻, OH⁻, and H₂O₂) actively guard bacteria in the host or function as signaling chemicals in various inflammatory illnesses or innate immune responses.¹ The complex antioxidant defense system, one of the primary adaptive strategies against pathogen invasion in fishes, can eliminate the overproduction of ROS. Microbial elicitors may promote oxidative bursts and accelerate the production of reactive oxygen species (ROS), which combat and kill invading microorganisms.² Nonetheless, the mass accumulation of ROS in vivo would reduce antioxidant defenses or cause oxidative damage to biological macromolecules, causing various disorders.³ Organisms have evolved complex and integrated antioxidant defense systems that include superoxide dismutases (SODs), cata-

lase (CAT), and different peroxidases to prevent the harmful effects of reactive oxygen species (ROS).⁴

SODs are essential for managing oxidative damage and the first line of defense against ROS.⁵ CAT converts superoxide radicals into less reactive H₂O₂, which is then catalyzed into H₂O by SODs.⁶ SODs typically consist of four varieties based on subcellular localization and bound iron: FeSOD, MnSOD, Cu/Zn-SOD, and NiSOD.⁷ MnSOD is particularly important for maintaining cellular homeostasis and removing excessive ROS from the host. CAT is essential for detoxifying H₂O₂ into the non-toxic end products H₂O and O₂.⁸ SOD and CAT can eliminate excessive ROS to maintain oxidation-antioxidation equilibrium and protect animals from oxidative injury.⁹ In addition, MnSOD and CAT can regulate mRNA transcription, which helps to understand the mRNA expressions of MnSOD and CAT to

a * Corresponding author. Hai Ren, E-mail: hairen1982@163.com

b * Corresponding author. Shaoyu Yang, E-mail: ysybt@126.com

Table 1. Primers used in this study

Primer name	Sequence (5'-3')	Usage	Size
SmMnSOD	F1-ATGCAGCTGCACCACAGCAA	Intermediate amplification	463 bp
	R3-CCARCCCCAGCCBGAGCCCTG		
	GSP-F1- CACCACAGCAAACACCACGCCACAT	5' and 3' end race amplification	
	GSP-R1- GCTCCATAGTCGTAGGTCAGGTCGG		
UPM	QF- CCGACCTGACCTACGACTATGGAG	MnSOD gene expression	162 bp
	QR- CAACCTGTGCCGTACGTCAC		
UPM	Long- CTAATACGACTCACTATAGGGCAAGCAG	5' and 3' end race amplification	
	Short- CTAATACGACTCACTATAGGGC		
CAT	QF- GATGTGGTCTTACCGACGAGATG	CAT gene expression	187 bp
	QR- CAGTGGAGAAGCGAATAGCGACAG		
β -actin	F- TAGGTGATGAAGCCCAGAGC	Internal reference gene expression	203 bp
	R- CTGGGTCATCTTCTCCCTGTT		

combat infections and provides fresh information regarding fish acclimation.

Since its introduction to Northern China in 1992, turbot (*Scophthalmus maximus*), one of the most frequent mariculture species with rapid growth and high resistance to low water temperatures, has been vital to fisheries' economic and aquaculture species. However, infections caused by bacteria, viruses, and parasites (such as *Vibrio anguillarum*, *nodavirus*, and *Philasterides dicentrarchi*) in booming turbot cultures have caused significant economic losses for the turbot business.¹⁰ According to reports, *V. anguillarum* is mainly responsible for severe infections in cultured turbot. Thus, additional research into the innate immune capabilities and the immune defense mechanism against *V. anguillarum* will contribute to disease control and turbot culture's chronic survival. This study aims to describe the nucleotide sequence of MnSOD from the liver of *S. maximus* in comparison to other known MnSODs, detect the expressions of MnSOD in various tissues, and quantify the expressions of MnSOD and CAT in response to *V. anguillarum*. Our findings would contribute to understanding the characteristics of MnSOD and CAT in fish.

MATERIALS AND METHODS

ANIMAL MATERIALS

Juvenile turbot weighing approximately 45.05±2.16 g were acquired from a farm in Changli, China. *Scophthalmus maximus* was first acclimated to the experimental conditions by spending one week in aerated, clean saltwater (salinity 19‰, 16±1 °C). Each group consisted of ten turbot and three fish tanks served as replicas. During the acclimation period, the turbot were fed twice daily with commercial pellets (vendor) with continuous oxygenation, and one-fourth of each tank's saltwater was replaced daily.

TOTAL RNA ISOLATION FROM TURBOT LIVER AND CDNA PREPARATION

Total liver RNA was isolated directly from healthy turbot using an RNAiso Plus system (TaKaRa, Japan). RNA's integrity and quantity/quality were then determined using agarose electrophoresis and an ND-1000UV (NanoDrop, USA) spectrophotometer, respectively. All extracted samples had an OD260/OD280 ratio between 1.8 and 2.0. Using M-MLV reverse transcriptase, first-strand cDNA was generated (TaKaRa). Using a SMART™ cDNA Kit, the 5' and 3' rapid amplification of cDNA end (RACE) cDNA templates were obtained (Clontech, USA). The manufacturer's instructions carried out all procedures.

CLONING OF *S. MAXIMUS* MNSOD

S. maximus MnSOD (SmMnSOD) full-length cDNA was produced using reverse-transcription polymerase chain reaction (RT-PCR) and RACE. The middle fragment of the SmMnSOD cDNA sequence was identified using degeneration primers F1 and R3 (Table 1) for the conserved regions and by aligning with the target genes of other fish species, including *Rachycentron canadum*, *Sparus aurata*, *Paralichthys olivaceus*, *Oplegnathus fasciatus*, *Anoplopoma fimbria*, and *Larimichthys crocea*. The PCR conditions were as follows: denaturation at 95°C for 5 minutes, followed by 33 cycles of denaturation at 95°C for 40 seconds, annealing at 56°C for 40 seconds, elongation at 72°C for 1 minute and 10 seconds, elongation at 72°C for 10 minutes, and storage at 4°C. Finally, a 463-bp fragment of MnSOD cDNA was amplified.

Using SMART™ RACE cDNA Kit, the 5' and 3' ends of the preceding SmMnSOD fragment sequence were obtained. The cDNA template derived from liver RNA, GSP-R1, and the anchor universal primer (UPM, Table 1) were utilized in the PCR of 5' end RACE. The GSP-F1 and the anchor UPM (Table 1) were selected for the 3' end of the RACE. In the SMART cDNA Kit manual, the PCR settings were specified.

The target band was excised and purified using a gel isolation kit (TaKaRa) before being subcloned into the pMD18-T cloning vector according to the manufacturer's instructions (TaKaRa) and transformed into competent *Escherichia coli* DH5. After PCR validation, Sangon Biotechnology Co., Ltd. sequenced the positive clones containing the DNA insert (Beijing, China).

SEQUENCE INVESTIGATION

The nucleotide and estimated amino acid sequences of SmMnSOD cDNA were compared using BLAST (<http://www.blast.ncbi.nlm.nih.gov/Blast>), SignalP 4.1 (<http://www.cbs.dtu.dk/services/SignalP/>), and ExPASy tools (<http://us.expasy.org/tools/>). DNAMAN was used for multiple alignment of the turbot MnSOD gene (Lynnon Biosoft, Canada). MEGA 11 software was used to create a phylogenetic tree of MnSOD, and statistical support for reliability was assessed using 1000 bootstrap replications.¹¹

DIFFERENTIAL EXPRESSIONS OF SMMNSOD DETECTED BY RT-QPCR

Primer Premier 5.0 was used to construct the qRT-PCR primers QF, QR, and -actin-F/R (**Table 1**) based on the SmMnSOD gene sequence and the internal housekeeping control gene β -actin (GenBank number: AY008305). Total RNA samples (1g) from healthy *S. maximus* tissues (gill, head, kidney, liver, stomach, muscle, heart, and intestine) were reverse-transcribed into cDNA using gDNA Eraser (TaKaRa) according to the manufacturer's protocol, and the expression levels of MnSOD mRNA transcript in each tested tissue were assessed using quantitative real time PCR (qRT-PCR).

EXPRESSION PATTERNS OF SMMNSOD AND CAT MRNA AFTER *V. ANGUILLARUM* INJECTION

The turbot was divided into two groups: test and control. Each turbot was injected intramuscularly with 100 μ L of a live bacterial suspension (2×10^7 CFU/mL) of *V. anguillarum* strains in the test group, which had been obtained from diseased *S. maximus* in Longxiang aquaculture farm (Laoting, China). Instead, sterile PBS was used in the control group. Following this treatment, the lives and kidneys of three turbot from each group were randomly taken at 3, 6, 12, 24, 48, and 72 h, and the samples were snap-frozen in liquid nitrogen for total RNA extraction and first-strand cDNA synthesis, as described above. Each time point was tested three times.

SmMnSOD and CAT (GenBank number: MG253621) post-injection expressions were detected using a CFX96 RT-PCR system (Bio-Rad, America) and SYBR green I. For SmMnSOD, a 162-bp PCR product was amplified using the gene-specific primers QF and QR. Still, for CAT, a 187-bp PCR product was amplified first with the specific primers QF and QR, and then the endogenous reference gene β -actin was amplified as a 203-bp product using the primers β -actin-F and β -actin-R (**Table 1**).

The cDNA was synthesized with a PrimeScript™ RT reagent kit with gDNA Eraser (TaKaRa, Japan) using 1 μ g of total RNA. The constructed cDNA was diluted 10-fold in DEPC water and stored at -70 °C for qRT-PCR. qRT-PCR was performed in triplicate in a total volume of 10 μ L, containing 1 \times SYBR Premix Ex Taq™ II (TaKaRa), 0.4 μ M of each primer, and 1 μ L of an RT solution. The settings for PCR amplification were provided in the manufacturer's instructions. Following each PCR thermal profile, the threshold cycle (C_T) was calculated using CFX96™ real-time PCR software 1.0 and applied to calculate the ΔC_T of each sample.¹² $2^{-\Delta\Delta C_T}$ was used to determine the relative expression of SmMnSOD and CAT.¹³

The mean, standard deviation (n=3) is presented for all experimental results. The qRT-PCR results were analyzed using a one-way analysis of variance (ANOVA) in SPSS 17.0 software. $P < 0.05$. was used as the significance level.

RESULTS

CHARACTERISTICS AND BIOINFORMATIC ANALYSIS OF SMMNSOD SEQUENCE

RACE-derived full-length SmMnSOD cDNA (**Figure 1**) was uploaded to the Genbank database (Accession Number: MG253620). As predicted by SignalP 4.1, the 1267-bp SmMnSOD cDNA has a 684-bp open reading frame (ORF) that encodes a 228-amino-acid protein with a 28-amino-acid signal peptide (**Figure 1**). The computed molecular mass of the protein was 23.87 kDa, and the theoretical isoelectric point was 6.75. The SmMnSOD amino acid sequence contained putative N-linked glycosylation sites of NVT, NHT, and NLS, as well as highly conserved signatures (DVWEHAYY).

HOMOLOGY ANALYSIS OF SMMNSOD

According to sequence analysis on the BLASTP, the deduced sequence of SmMnSOD had the same consensus pattern as the MnSODs of vertebrates and had an overall identity of 85.3 % to 92.9 % with eight different known MnSOD members (**Figure 2**). The highest identity was observed with homologs from *Oplegnathus fasciatus* and *Rachycentron canadum*, with 92.9 % identity.

PHYLOGENETIC ANALYSIS

The identification and phylogeny of SmMnSOD were confirmed further using a phylogenetic tree constructed on MEGA 11 using the sequences of the selected MnSODs (**Figure 3**). The MnSOD gene family is thought to be divided into two primary phylogenetic clusters. The SmMnSOD was similar to some fish species but not to *Homo sapiens*, *Gallus gallus*, *Melopsittacus undulatus*, or *Mus musculus* MnSODs (**Figure 3**).

BASAL TISSUE EXPRESSION OF SMMNSOD MRNA

SmMnSOD gene expression patterns were studied in seven different tissue types of healthy turbot, including the gills,

```

1 AC ATG GGG GAG TTA TCA TCA TCA TCA GCA CGT CTC TCC GGT CCC GCG GCC ACT GTC GTG 59
   M G E L S S S S A R L S G P A A T V V
60 AAC ATG CTT TGC AGA GTT GGT CAA ATG CGC AGG TGT GCA GCC ACC CTC AGC CAA TCT ATA 119
   N M L C R V G Q M R R C A A T L S Q S I
120 AAC CAG GCA GCA GCA GCA GCA GCG AGG CAC AAG CAC ACG CTC CCC GAC CTG ACC TAC GAC 179
   N Q A A A A A A R H K H T L P D L T Y D
180 TAT GGA GCC CTG GAG CCC AGC ATC AAC GCG GAG ATT ATG CAG CTG CAC CAC AGC AAA CAC 239
   Y G A L E P S I N A E I M Q L H H S K H
240 CAC GCC ACA TAT GTC AAC AAC CTC AAC GTG ACC GAG GAG AAA TAT CAA GAG GCG CTG GCA 299
   H A T Y V N N L N V T E E K Y Q E A L A
300 AAG GGT GAC GTG ACG GCA CAG GTT GCC CTC CAG CCG GCT CTG AGG TTT AAC GGG GGA GGC 359
   K G D V T A Q V A L Q P A L R F N G G G
360 CAC GTT AAT CAC ACT ATC TTC TGG ACC AAT CTT TCT CCA AAC GGC GGA GAC GAG CCA CAG 419
   H V N H T I F W T N L S P N G G D E P Q
420 GGG GAG CTA ATG GAA GCC ATC AAG CGG GAC TTT GGC TCC TTC CAG ACA ATG AAA GAG AAG 479
   G E L M E A I K R D F G S F Q T M K E K
480 ATG TCC GGC GCC ACC GTG GCG GTG CAG GGC TCA GGC TGG GGT TGG CTG GGC TAT GAC AAG 539
   M S A A T V A V Q G S G W G W L G Y D K
540 GAG AGT GGA CGA CTC CGC GTC GCT GCT TGT TCA AAC CAG GAT CCT CTG CAG GGG ACA ACA 599
   E S G R L R V A A C S N Q D P L Q G T T
600 GGT CTC ATC CCT CTC CTT GGT ATT GAT GTA TGG GAG CAC GCC TAC TAC CTT CAG TAC AAA 659
   G L I P L L G I D V W E H A Y Y L Q Y K
660 AAT GTG CGG CCG GAC TAT GTT AAA GCT ATC TGG AAT GTG ATC AAC TGG GAG AAT GTG ACT 719
   N V R P D Y V K A I W N V I N W E N V T
720 GAG CGT CTT CAA TCA GCC AAA AAG TAC AACCCCTAACC TCAGACATCC CCAACAACCC GTCOCATCCC 786
   E R L Q S A K K *
787 CGATCAAAGA GAAGTTGCAA AAAATTCTTA GTTTTACATT GCATGTCATG TCAATGATAA TGATAATGAT 856
857 AATGTTTTTG GAATTCGAGA TGGTTCACCT GCATTCAAGT TGCTTCCACT GACTTTGAAA ATACTCTCTT 926
927 TAITGTTGCA GATTACATTG TCCTTATGGG GAAAAATGC ACAAGTTGAA GCAAAATTAA AAATCATTTG 996
997 CAAGTGCCCT TTAATCTCAG ATCTTCCCTC AACCAACCAGA CTTATTTTCA AGCGCACAAA AAATAGCCAA 1066
1067 GTTCCAAGTG AAAGGCTGGC TTTTATTTAT CTCACTGAAA TAACTGCTGA CATATTCGTT GGCACATAAC 1136
1137 CAGAGGGCAT ATTCACTGTC AGAATAATCC AACTGAAAAG CAATGTTATT GCAGTCCCAT GTTATTGATG 1206
1207 TATTATAATA AAGTTATAGG ATTTCACTGG TAAAAAATAA AAAAAAATAA AAAAAAATAA A 1267

```

Figure 1. Nucleotide sequence of *S. maximus* MnSOD cDNA and deduced amino acid sequence

Underlining: amino acid sequence of signal peptide; oval: start codon (ATG), stop codon (TAG); Double underlining: polyadenylating signal sequence (ATAAA); boxing: conserved signature motifs (DVWEHAYY); gray shading: structural domains.

stomach, liver, head, kidney, intestine, heart, and muscle (Figure 4). SmMnSOD and β -actin dissociation curves only showed one peak, indicating that the amplifications were unique. The results showed SmMnSOD expression was highest in the liver, lowest in the muscle, and moderate in the other tissues (Figure 4).

EXPRESSION PROFILES OF SMMNSOD AFTER *V. ANGUILLARUM* CHALLENGE

The transcript levels of SmMnSOD in the liver and head kidney following *V. anguillarum* infection were measured using qRT-PCR with the β -actin gene as the endogenous reference. Compared to the control group, SmMnSOD transcript levels increased considerably in the liver from 12 to 72 hours ($P < 0.05$), maximized at 24 hours with an 8.9-fold increase for the challenge group (Figure 5a).

SmMnSOD mRNA expression in the test group's head kidney declined quickly after the challenge, and was significantly lower than in the control group during the first 12 hours ($P < 0.05$; Figure 5b). Following that, SmMnSOD mRNA expression increased progressively in the challenge group, maximized at 48 h with a 2.3-fold increase relative to the control group ($P < 0.05$), and subsequently decreasing to 1.29-fold at 72 h ($P > 0.05$) (Figure 5b).

EXPRESSION PROFILES OF CAT AFTER *V. ANGUILLARUM* CHALLENGE

Figure 6 shows the CAT expression profiles following pathogenic infection. In the challenge group, CAT expression in the liver of *S. maximus* increased steadily from 3 to 48 h, maximized at 48 h with a 4.17-fold increase compared to the control group ($P < 0.05$). The CAT transcript level in the liver then reduced after 72 hours but remained significantly

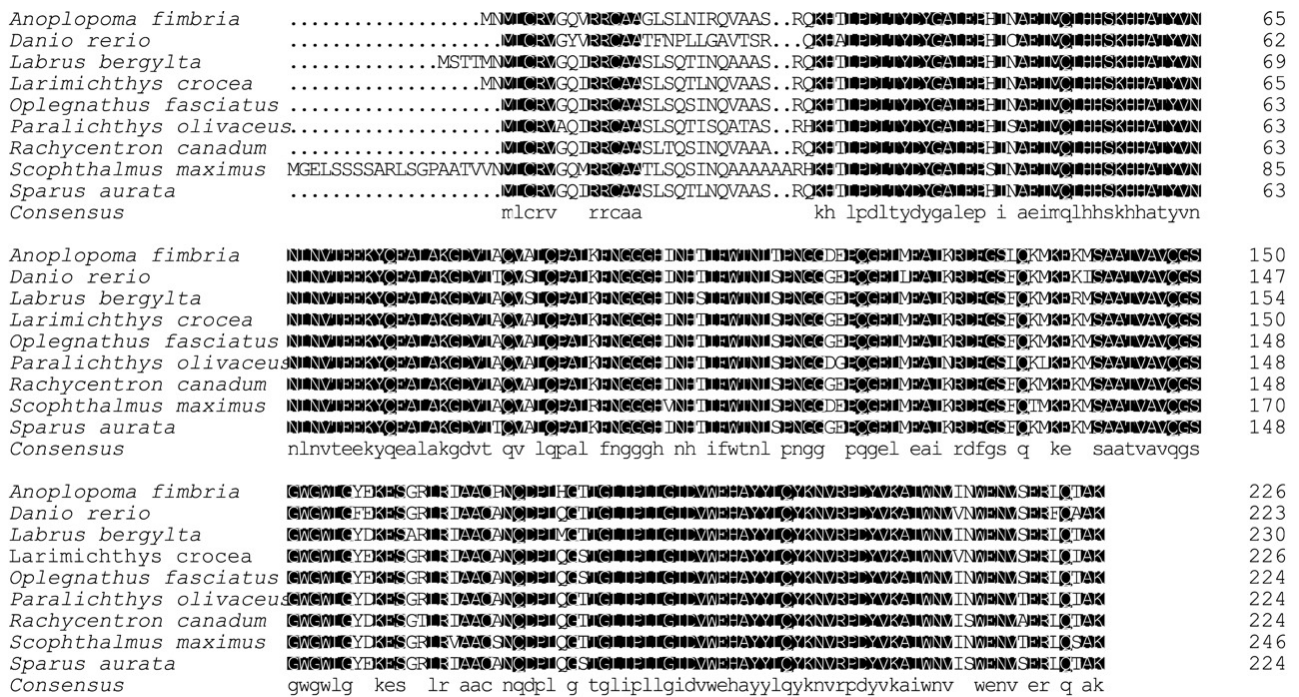


Figure 2. Multiple alignments of deduced amino acid sequence of SmMnSOD and other known MnSODs

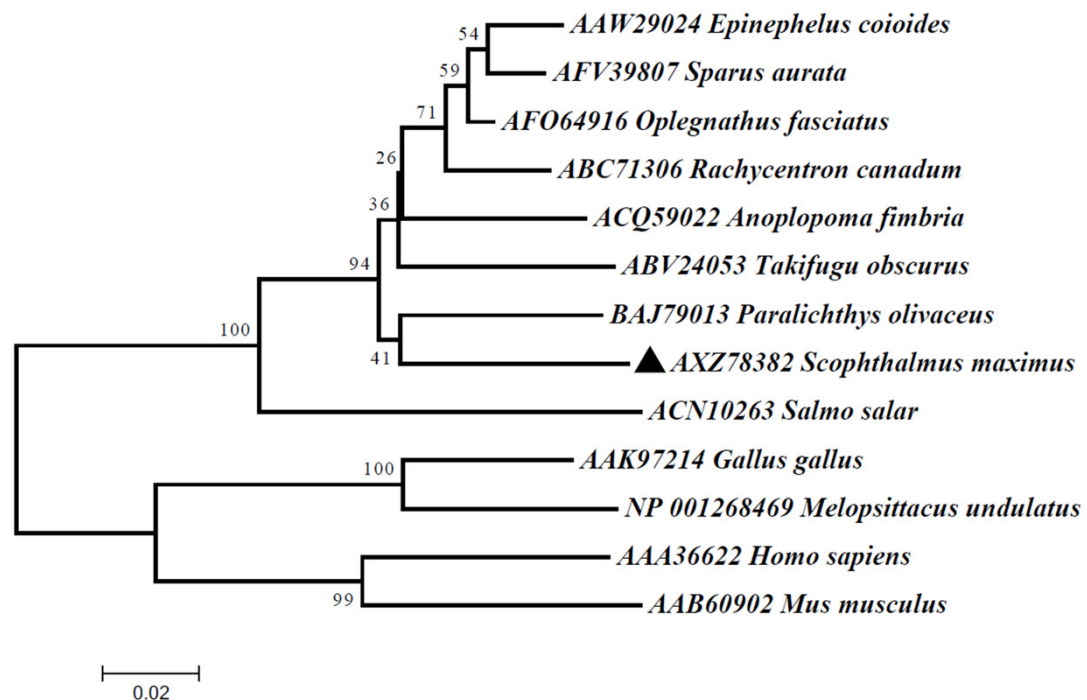


Figure 3. Phylogenetic tree of amino acid sequences of MnSOD from different species

more significant than in the control group ($P < 0.05$; Figure 6a).

Within the first 6 hours, the CAT transcript level in the head kidney of *S. maximus* was significantly lower than the control group ($P < 0.05$). The CAT expression level then steadily increased in the challenge group, although it increased significantly from 24 to 72 h, maximized at 48 h by 1.59-fold compared to the control group ($P < 0.05$; Figure 6b).

DISCUSSION

SODs are important metalloenzymes in antioxidant defense pathways that reduce ROS buildup and free-radical-caused cell damage in vivo.¹⁴ SODs are the first line of defense against oxidative stress caused by massive ROS levels in the body. In this article, for the first time, a novel 1267-bp full-length MnSOD gene was isolated and described from *S.*

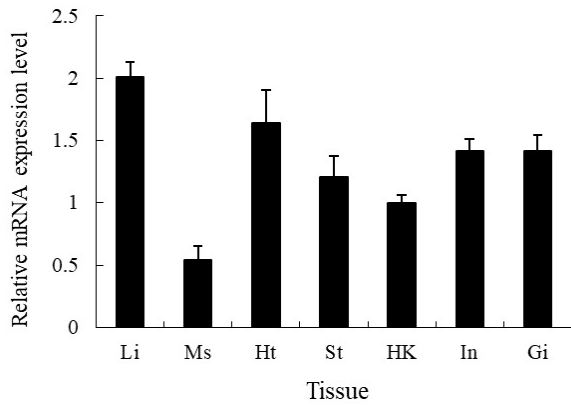


Figure 4. Relative transcript levels of SmMnSOD in Li (liver), Ms (muscle), Ht (heart), St (stomach), HK (head kidney), In (intestine), and Gi (gill) determined by qRT-PCR.

maximus, and it showed high similarity (85.3 % - 92.9 %) with MnSODs from other animals. Multiple sequence alignment revealed that the SmMnSOD hallmark motifs (DVWE-HAYY) were substantially conserved in species¹⁵ (Figure 2). Phylogenetic research revealed that SmMnSOD belonged to the fish SOD family and clustered with fish homologs. The presence of MnSODs in animals shows that MnSODs have a common ancestor and are conserved during evolution. The SmMnSOD belongs to the MnSOD family based on its close relationship with other fishes.

SmMnSOD was shown to be expressed in all turbot tissues tested using qRT-PCR. The SmMnSOD transcript expression was highest in the liver, which is consistent with previous findings in *Megalobrama amblycephala*,¹⁶ *Hypophthalmichthys molitrix*,¹⁷ and *Hemibarbus mylodon*.^{17,18} However, this contradicts another finding showing MnSOD expression is highest in the heart of *Sebastes schlegelii*.¹⁹ Furthermore, the lowest expression level in muscle in our investigation contradicts *Hemibarbus mylodon*.¹⁸ MnSOD

expression patterns in fish may be attributed to the tissue dependence on mitochondrial and oxidative levels, as MnSOD primarily deletes ROS generated during mitochondrial respiration.¹⁸ According to findings, antioxidant enzymes are expressed at the mRNA level in the liver of many fish species.²⁰ SmMnSOD transcript levels are highest in the liver, most likely due to oxidative reactions and highly metabolic antioxidant defenses that always occur in the liver.²¹ These findings indicate that MnSOD in the liver plays a vital role in antioxidant defenses.

Virulent pathogens have a significant impact on aquaculture development. The experimental challenge of pathogen bacteria significantly affects MnSOD expression in *Takifugu obscurus*, *Pseudosciaena crocea*, *Hemibarbus mylodon*, *Procambarus clarkia*, *Crassostrea hongkongensis*, and *Meretrix meretrix*. *V. anguillarum*, a significant pathogen bacterium, is said to cause severe infections and widespread mortality in farmed marine fishes.²² There has yet to be any research on the effect of *V. anguillarum* on MnSOD expression in one of its most heavily attacked species, *S. maximus*.²³

Since the liver and kidney are the primary sites of oxidative reactions and antioxidant defenses,²⁴ determining the MnSOD gene expression levels in these two tissues following *V. anguillarum* infection provide more insight into its immunological function. According to our findings, Live *V. anguillarum* strongly activated MnSOD in the liver and head kidney of *S. maximus*. SmMnSOD expression increased considerably after 48 h in the test group against the control group, which might be attributable to the ROS stress generated by *V. anguillarum* infection, indicating that SmMnSOD is engaged in antioxidant defense and can be induced when infected with *V. anguillarum*. SmMnSOD expression in the liver and head kidney gradually decreased at 24 and 48 hours, respectively. MnSOD transcription was inhibited in the challenged group, most likely because the continuous reproduction of viable *V. anguillarum* in hosts created severe cytotoxic effects and severely impaired nor-

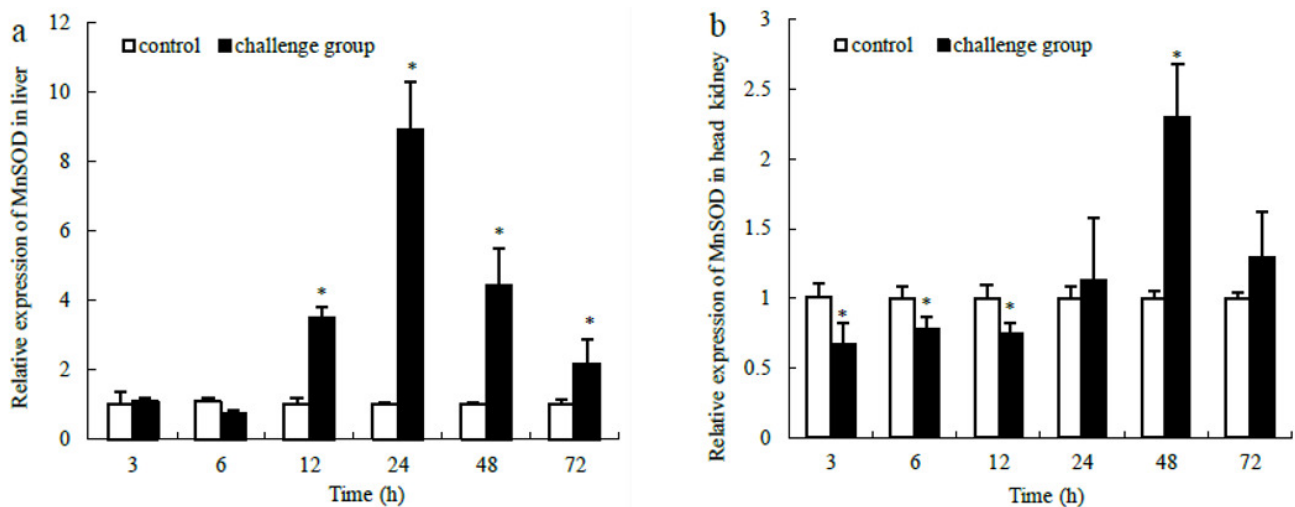


Figure 5. Transcript levels of SmMnSOD in the liver (a) and the head kidney (b) of *S. maximus* after the bacterial challenge detected by qRT-PCR

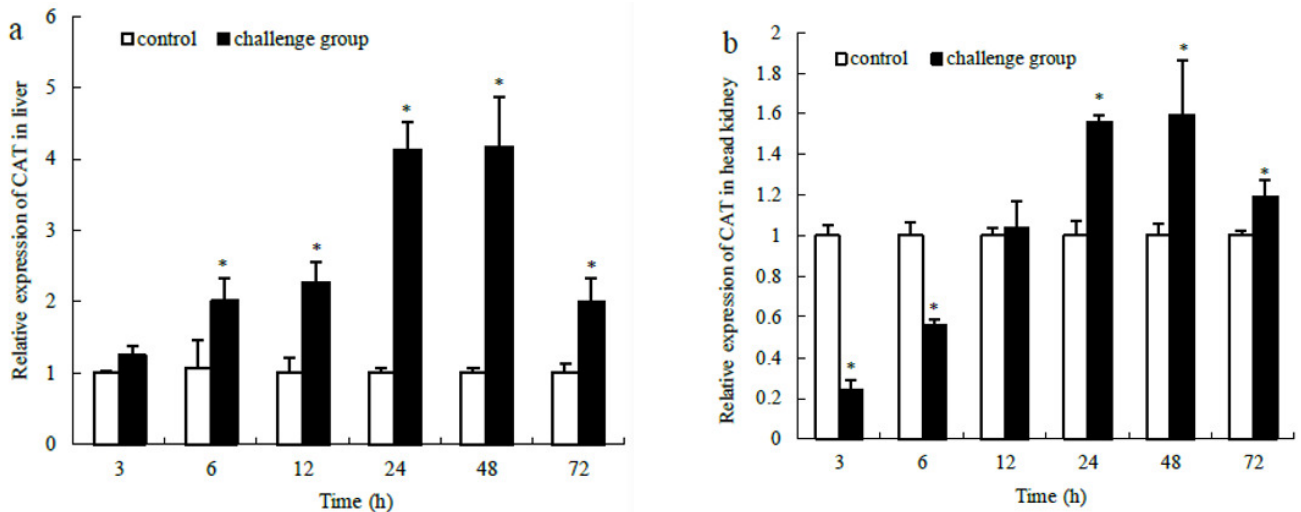


Figure 6. Transcript levels of CAT in the liver (a) and the head kidney (b) of *S. maximus* after the bacterial infection as detected by qRT-PCR

mal cell function, resulting in either apoptosis or cell-function loss.^{25,26}

These findings suggest that MnSOD may play a role in the immunological response against *V. anguillarum* infection. We also found that MnSOD expression patterns differed between the liver and the head kidney, most likely due to the antioxidant defense system's various cell and tissue activities.²⁷ Another MnSOD expression investigation from *Carassius auratus* yielded similar results.²⁸ The transcript profile analysis in our study shows that pathogenic bacteria can induce MnSOD, implying that MnSOD plays an essential role in *S. maximus*' antioxidant defense response. Because MnSOD is a component of the antioxidant system, monitoring its expression alone cannot provide a complete picture of the oxidative stress caused by pathogenic bacteria. Thus, additional CAT research is required for ecotoxicity monitoring. The explanation is that SOD and CAT mitigate the adverse effects of ROS by converting them into O₂ and H₂O, thereby protecting organisms from lipid peroxidation and balancing cellular redox reactions.^{17,29}

Past studies have shown that pathogenic bacteria such as *Vibrio alginolyticus*, *Streptococcus iniae*, and *V. alginolyticus* can produce CAT quickly. In our study, *V. anguillarum* dramatically increased CAT mRNA transcription levels in the liver and head kidney at 6 and 24 h, respectively, peaked at 48 h, and then progressively reduced, indicating that CAT was inducible and likely participates in antipathogenic immunological reactions in *S. maximus*. Unfortunately, it has not yet been determined why the induction of MnSOD and CAT by *V. anguillarum* challenge is more significant in the liver than in the head kidney. One probable explanation is that the liver is the principal organ involved in oxidative reactions and antioxidative defenses.¹⁸ Nonetheless, more research is needed to determine the precise mechanism of bacterial infection on antioxidant genes in *S. maximus*.

In summary, MnSOD was identified in *S. maximus* for the first time, and it was found to be constitutively expressed in the liver (highest), gills, stomach, head-kidney, muscle, intestine, and heart. MnSOD and CAT expressions in the

liver and head kidney following *V. anguillarum* challenge revealed that MnSOD and CAT were inducible and may have engaged in the innate immune response of fishes against pathogenic infection. This study provides some fresh and significant evidence for further research into the regulatory mechanism of the antioxidant defense system against infections in flounder fishes.

ACKNOWLEDGMENTS

Financial support from the National Natural Science Foundation of China (31502187), the Major Science and Technology Projects of Hebei Province (20286701Z), the Natural Science Foundation of Hebei Province (C2018407049), Science and Research Funds of Hebei Normal University of Science and Technology (2020YB008), the Science and Technology Projects of Hebei Province (20567621H) are gratefully acknowledged. The authors thank EditSprings (<https://www.editsprings.cn>) for the expert linguistic services provided.

DECLARATION OF COMPETING INTEREST

The authors have stated that no competing interests exist.

AUTHORS' CONTRIBUTION - CREDIT

Conceptualization: Hai Ren (Equal), Shaoyu Yang (Equal). Methodology: Hai Ren (Lead), Jing Mei (Supporting). Formal Analysis: Hai Ren (Lead). Investigation: Hai Ren (Lead). Writing – original draft: Hai Ren (Lead). Funding acquisition: Hai Ren (Lead). Writing – review & editing: Qinglin Wang (Supporting), Xiaomin Jin (Supporting), Guisheng Gao (Equal). Resources: Guoshan Qi (Equal), zenping He (Equal). Supervision: Shaoyu Yang (Lead).

Submitted: February 15, 2023 CDT, Accepted: June 27, 2023

CDT



This is an open-access article distributed under the terms of the Creative Commons Attribution 4.0 International License (CCBY-NC-ND-4.0). View this license's legal deed at <https://creativecommons.org/licenses/by-nc-nd/4.0> and legal code at <https://creativecommons.org/licenses/by-nc-nd/4.0/legalcode> for more information.

REFERENCES

1. Eckersall PD, Bell R. Acute phase proteins: Biomarkers of infection and inflammation in veterinary medicine. *The Veterinary Journal*. 2010;185(1):23-27. doi:10.1016/j.tvjl.2010.04.009
2. Levine A, Tenhaken R, Dixon R, Lamb C. H2O2 from the oxidative burst orchestrates the plant hypersensitive disease resistance response. *Cell*. 1994;79(4):583-593. doi:10.1016/0092-8674(94)90544-4
3. Zabaleta I, Bizkarguenaga E, Bilbao D, Etxebarria N, Prieto A, Zuloaga O. Fast and simple determination of perfluorinated compounds and their potential precursors in different packaging materials. *Talanta*. 2016;152:353-363. doi:10.1016/j.talanta.2016.02.022
4. Parolini M, Magni S, Castiglioni S, Binelli A. Amphetamine exposure imbalanced antioxidant activity in the bivalve *Dreissena polymorpha* causing oxidative and genetic damage. *Chemosphere*. 2016;144:207-213. doi:10.1016/j.chemosphere.2015.08.025
5. Bruno-Bárcena JM, Andrus JM, Libby SL, Klaenhammer TR, Hassan HM. Expression of a heterologous manganese superoxide dismutase gene in intestinal Lactobacilli provides protection against hydrogen peroxide toxicity. *Appl Environ Microbiol*. 2004;70(8):4702-4710. doi:10.1128/aem.70.8.4702-4710.2004
6. Mruk DD, Silvestrini B, Mo MY, Cheng CY. Antioxidant superoxide dismutase - a review: its function, regulation in the testis, and role in male fertility. *Contraception*. 2002;65(4):305-311. doi:10.1016/s0010-7824(01)00320-1
7. Kim EJ, Chung HJ, Suh B, Hah YC, Roe JH. Transcriptional and post-transcriptional regulation by nickel of *sodN* gene encoding nickel-containing superoxide dismutase from *Streptomyces coelicolor* Müller. *Molecular microbiology*. 1998;27(1):187-195. doi:10.1046/j.1365-2958.1998.00674.x
8. Nordberg J, Arnér ESJ. Reactive oxygen species, antioxidants, and the mammalian thioredoxin system. *Free Radical Biology and Medicine*. 2001;31(11):1287-1312. doi:10.1016/s0891-5849(01)0724-9
9. Bagnyukova TV, Storey KB, Lushchak VI. Induction of oxidative stress in *Rana ridibunda* during recovery from winter hibernation. *Journal of Thermal Biology*. 2003;28(1):21-28. doi:10.1016/s0306-4565(02)00031-1
10. Yang CG, Wang XL, Wang L, Zhang B, Chen SL. A new Akirin1 gene in turbot (*Scophthalmus maximus*): Molecular cloning, characterization and expression analysis in response to bacterial and viral immunological challenge. *Fish & Shellfish Immunology*. 2011;30(4-5):1031-1041. doi:10.1016/j.fsi.2011.01.028
11. Tamura K, Dudley J, Nei M, Kumar S. MEGA 4: molecular evolutionary genetics analysis (MEGA) software version 4.0. *Molecular Biology and Evolution*. 2007;24(8):1596-1599. doi:10.1093/molbev/msm092
12. Rhee JS, Won EJ, Kim RO, Lee J, Shin KH, Lee JS. Expression of superoxide dismutase (SOD) genes from the copper-exposed polychaete, *Neanthes succinea*. *Marine Pollution Bulletin*. 2011;63(5-12):277-286. doi:10.1016/j.marpolbul.2011.04.023
13. Livak KJ, Schmittgen TD. Analysis of relative gene expression data using real time quantitative PCR and the 2- $\Delta\Delta$ CT method. *Methods*. 2001;25(4):402-408. doi:10.1006/meth.2001.1262
14. Umasuthan N, Bathige SD, Revathy KS, et al. manganese superoxide dismutase (MnSOD) from *Ruditapes philippinarum*: comparative structural- and expressional-analysis with copper zinc superoxide dismutase (Cu/ZnSOD) and biochemical analysis of its antioxidant activities. *Fish & Shellfish Immunology*. 2012;33(4):753-765. doi:10.1016/j.fsi.2012.06.024
15. Ren H, Li J, Li J, Liu P, Liang Z, Wu J. Transcript profiles of mitochondrial and cytoplasmic manganese superoxide dismutases in *Exopalaemon carinicauda* under ammonia stress. *Chin J Ocean Limnol*. 2015;33(3):714-724. doi:10.1007/s00343-015-4143-5
16. Sun S, Zhu J, Jiang X, Li B, Ge X. Molecular cloning, tissue distribution and expression analysis of a manganese superoxide dismutase in blunt snout bream *megalobrama amblycephala*. *Fish & Shellfish Immunology*. 2014;38(2):340-347. doi:10.1016/j.fsi.2014.03.036
17. Zhang ZW, Li Z, Liang HW, Li L, Luo XZ, Zou GW. Molecular cloning and differential expression patterns of copper/zinc superoxide dismutase and manganese superoxide dismutase in *Hypophthalmichthys molitrix*. *Fish & Shellfish Immunology*. 2011;30(2):473-479. doi:10.1016/j.fsi.2010.11.003

18. Cho YS, Lee SY, Bang IC, Kim DS, Nam YK. Genomic organization and mRNA expression of manganese superoxide dismutase (Mn-SOD) from *Hemibarbus mylodon* (Teleostei, Cypriniformes). *Fish & Shellfish Immunology*. 2009;27(4):571-576. doi:10.1016/j.fsi.2009.07.003
19. Perera NCN, Godahewa GI, Nam BH, Park JY, Lee J. Two metalloenzymes from rockfish (*Sebastes schlegelii*): Deciphering their potential involvement in redox homeostasis against oxidative stress. *Fish & Shellfish Immunology*. 2018;80:31-45. doi:10.1016/j.fsi.2018.05.050
20. Kim JH, Rhee JS, Lee JS, et al. Effect of cadmium exposure on expression of antioxidant gene transcripts in the river pufferfish, *Takifugu obscurus* (Tetraodontiformes). *Comparative Biochemistry and Physiology Part C*. 2010;152(4):473-479. doi:10.1016/j.cbpc.2010.08.002
21. Avci A, Kaçmaz M, Durak İ. Peroxidation in muscle and liver tissues from fish in a contaminated river due to a petroleum refinery industry. *Ecotoxicology and Environmental Safety*. 2005;60(1):101-105. doi:10.1016/j.ecoenv.2003.10.003
22. Planas M, Pérez-Lorenzo M, Vázquez JA, Pintado J. A model for experimental infections with *Vibrio (Listonella) anguillarum* in first feeding turbot (*Scophthalmus maximus* L.) larvae under hatchery conditions. *Aquaculture*. 2005;250(1-2):232-243. doi:10.1016/j.aquaculture.2005.04.050
23. Chair M, Dehasque M, Van Poucke S, Nelis H, Sorgeloos P, De Leenheer AP. An oral challenge for turbot larvae with *Vibrio anguillarum*. *Aquacult Int*. 1994;2(4):270-272. doi:10.1007/bf00123437
24. Velma V, Tchounwou PB. Hexavalent chromium-induced multiple biomarker responses in liver and kidney of goldfish, *Carassius auratus*. *Environ Toxicol*. 2011;26(6):649-656. doi:10.1002/tox.20602
25. Lee SJ, Lim KT. UDN glycoprotein regulates activities of manganese-superoxide dismutase, activator protein-1, and nuclear factor- κ B stimulated by reactive oxygen radicals in lipopolysaccharide-stimulated HCT-116 cells. *Cancer Letters*. 2007;254(2):274-287. doi:10.1016/j.canlet.2007.03.009
26. Duan Y, Li J, Zhang Z, Li J, Ge Q, Liu P. The role of oncoprotein NM23 gene from *Exopalaemon carinicauda* in response to pathogens challenge and ammonia-N stress. *Fish & Shellfish Immunology*. 2015;47(2):1067-1074. doi:10.1016/j.fsi.2015.08.018
27. Tian J, Chen J, Jiang D, Liao S, Wang A. Transcriptional regulation of extracellular copper zinc superoxide dismutase from white shrimp *Litopenaeus vannamei* following *Vibrio alginolyticus* and WSSV infection. *Fish & Shellfish Immunology*. 2007;30(1):234-240. doi:10.1016/j.fsi.2010.10.013
28. Dan Q. *The Copper Zinc Superoxide Dismutase and Manganese Superoxide Dismutase from Qihe Crucian Carp Carassius Auratus: Molecular Cloning, Characterization and Response to Aeromonas Hydrophila Infection*. Henan Normal University; 2015.
29. Chen P, Li J, Liu P, Gao B, Wang Q, Li J. cDNA cloning, characterization and expression analysis of catalase in swimming crab *Portunus trituberculatus*. *Mol Biol Rep*. 2012;39(12):9979-9987. doi:10.1007/s11033-012-1826-2